Long-term trends in urban NO_2 concentrations and associated pediatric asthma cases: estimates from global datasets

Susan C. Anenberg[1*], Arash Mohegh[1*], Daniel L. Goldberg[1,2], Michael Brauer[3,4], Katrin Burkart[3], Perry Hystad[5], Andrew Larkin[5], Sarah Wozniak[3], Lok Lamsal[6]

1 Milken Institute School of Public Health, George Washington University, Washington, DC, USA

2 Energy Systems Division, Argonne National Laboratory, Washington, DC, USA

3 Institute for Health Metrics and Evaluation, University of Washington, Seattle, Washington, USA

4 University of British Columbia, Vancouver, BC, Canada

5 Oregon State University, Corvallis, OR, USA

6 NASA Goddard Space Flight Center, Greenbelt, MD, USA

* These authors contributed equally to this work.

Corresponding author: Susan Anenberg, 950 New Hampshire Ave NW, Washington, DC 20052, sanenberg@gwu.edu, 1-202-994-2392

Abstract

Background: Levels of nitrogen dioxide (NO_2), a combustion-related air pollutant largely associated with traffic in urban areas, have been changing rapidly due to competing influences of regulation and population and fossil fuel-powered economic expansion. Traffic-related NO_2 is associated with pediatric asthma incidence in epidemiological studies around the world. We aim to assess long-term trends in NO_2 concentrations and NO_2-attributable pediatric asthma incidence in cities globally.

Methods: We estimate global annual average surface NO_2 concentrations at 1km resolution for 1990-2019 by combining land use regression model predictions with NO_2 column densities from the Ozone Monitoring Instrument satellite sensor. We use these concentrations with an epidemiologically-derived concentration-response factor, population, and baseline disease rates to estimate NO_2-attributable pediatric asthma incidence. We explore trends over the last two decades.

Findings: We found diverging regional trends leading to an emerging global convergence in urban NO_2 concentrations globally from 2000-2019. Concentrations are high but declining in high-income countries and low but rising elsewhere. Estimated NO_2-attributable pediatric asthma incidence shows similar trends with decreases of 28-56% in North America, Western and Central Europe, and Australasia, but increases of >50% in Central and South Asia and >100% in Sub-Saharan Africa.

Interpretation: Traffic-related air pollution continues to be an important contributor to pediatric asthma incidence in cities in both developed and developing countries. Divergent experiences of different world regions show that while population growth is worsening NO_2 levels with substantial implications for

children's health in Asia and Africa, rapid and substantial NO_2 declines are possible with effective regulations.

Funding: Health Effects Institute and NASA

Research in context:

Evidence before this study: We searched PubMed and Google Scholar databases for studies published in English from the database inception until March 11, 2021, using the search terms ("NO_2" OR "nitrogen dioxide") AND "asthma" AND "trends". Previous studies have reported epidemiological analyses linking changes with asthma to changes in NO_2, or have assessed long-term trends in NO_2 concentrations in some countries or world regions. However, these studies provide little information about how NO_2 concentrations are changing in urban areas all around the world, and the influence those changes have on pediatric asthma incidence. One study published in 2019 showed that over 4 million new pediatric asthma cases, representing ~13% of all pediatric asthma cases worldwide in 2015, could be attributed to NO_2 pollution. Understanding temporal trends in NO_2-attributable pediatric asthma incidence could help inform asthma and air pollution mitigation strategies.

Added value of this study: To our knowledge, this is the first study to have estimated long-term trends in NO_2 concentrations and NO_2-attributable pediatric asthma incidence in urban areas worldwide. We focus on the last two decades, from 2000 to 2019, a period in which NO_2 levels have been changing rapidly around the world due to competing influences of regulation versus population growth and fossil fuel-powered economic expansion. We show that regional trends are diverging, with high but declining concentrations in high-income countries that have regulated NO_2 and low but rising concentrations in other parts of the world where population is expanding. The effect of these contrasting trends is an emerging convergence in urban NO_2 concentrations, and, to a lesser extent, NO_2-attributable asthma incidence, globally.

Implications of all the available evidence: Urban NO_2 concentrations have been trending downward for decades in places that have effective air quality regulations, with benefits for improved children's respiratory health. Even with these improvements, the current levels of NO_2 contribute substantially to pediatric asthma incidence, highlighting that mitigating air pollution should be a critical element of children's public health strategies. For cities that have not benefited from strong local or national air quality management programs, the experience of cities that have such programs demonstrates that addressing combustion-related air pollution can lead to dramatic improvements in air quality and public health over short time frames. Our study also demonstrates the utility of satellite remote sensing for environmental and public health surveillance in urban areas worldwide.

Acknowledgements: This work was supported by grants from the Health Effects Institute (Research Agreement #4977/20-11) and NASA (Grant #80NSSC19K0193). We gratefully acknowledge the developers of the OMI NO_2 concentration products, GHS-SMOD urban area dataset, GBD disease rate datasets, and Worldpop population dataset. We appreciate helpful discussions with Bryan Duncan. Research described in this article was conducted under contract to the Health Effects Institute (HEI), an organization jointly funded by the United States Environmental Protection Agency (EPA) (Assistance Award No. R-82811201) and certain motor vehicle and engine manufacturers. The contents of this

article do not necessarily reflect the views of HEI, or its sponsors, nor do they necessarily reflect the views and policies of the EPA or motor vehicle and engine manufacturers.

Data availability: NO_2 concentrations are available at: https://figshare.com/articles/dataset/Global_surface_no2_concentrations_1990-2020/12968114. Estimated NO_2-attributable asthma incidence results are available at: https://github.com/AMohegh/Asthma_no2_urban

Author contributions: SCA, AM, and DG designed the study; PH, AL, and LL provided data; AM carried out the calculations, SCA, AM, DG, MB, PH, AL, and SW contributed input on methods development; SCA and AM wrote the paper; all authors helped interpret results and reviewed the manuscript. AM and DG have verified the underlying data.

Declaration of interests: The authors declare no conflict of interest.

Introduction

Nitrogen dioxide (NO_2), a component of nitrogen oxides (NO_x), is a pervasive air pollutant that is regulated by the U.S. Environmental Protection Agency. NO_2 is a precursor for ground-level ozone and fine particulate matter ($PM_{2.5}$), other regulated air pollutants that are the leading contributors to air pollution-related mortality.[1] NO_2 is an effective tracer for anthropogenic fuel combustion generally, and traffic specifically.[2–5] Major anthropogenic NO_2 sources include on-road and non-road transportation tailpipe emissions (including heavy-, medium-, and light-duty vehicles, shipping, and aviation), power plants, industrial manufacturing, and agriculture.[6–9] In urban and industrialized areas, a lower fraction of NO_2 comes from natural sources like soil and lightning. NO_2 concentration trends can be used to evaluate the efficacy of air pollution regulations, as well as effects of abrupt emission changes (e.g. power plant closures, new oil and gas fields, COVID-19 lockdowns).[10–13]

In addition to its role in $PM_{2.5}$ and ozone formation, NO_2 itself (often as a marker for the broader traffic-related air pollution mixture) has been linked to several adverse health outcomes including asthma exacerbation.[14,15] Recent epidemiological studies have also found associations between transportation related air pollutants with new asthma development in children.[16,17] While the putative agent in the traffic-related air pollution mixture remains unknown, epidemiological studies are relatively consistent in their finding that NO_2 is significantly associated with pediatric asthma incidence, while the evidence for other traffic-related air pollutants (e.g. $PM_{2.5}$) is more mixed.[16,17] Previous health impact assessments have linked NO_2 with over four million new pediatric asthma cases each year globally, ~13% of the global pediatric asthma burden.[18,19] The fraction of new pediatric asthma cases that were attributed to NO_2 ranged substantially higher, up to ~50%, in urban areas.

NO_x emissions and NO_2 concentrations have changed dramatically in response to socioeconomic changes.[20–24] In the U.S., NO_2 concentrations have dropped ~50% on average from the 1980s to 2010s,[25] with even larger drops near major roadways[25] and point sources.[10] In the last two decades, U.S. NO_x emissions have been falling ~5% per year as vehicles get more fuel efficient and cleaner and as power plants have been shifting from coal to relatively cleaner fuels (e.g. natural gas).[11,26,27] NO_2 concentrations have also decreased in Europe, though more slowly.[28,29] In contrast, NO_2 has been increasing in India,[30] the Middle East,[31] and eastern Europe.[22] In China, NOx emissions peaked around 2011/2012 and subsequently declined.[32–34]

Previous research on NO_2 temporal trends in urban areas have focused only on a small subset of cities and have not considered its health impacts, precluding the ability to compare urban trends in NO_2 concentrations and associated health burdens in a consistent manner across the world. The global coverage and long continuous record of satellite remote sensing since the 1990s make it possible to track urban NO_2 concentrations globally.[35–38] Additionally, current satellite instruments operate with substantially higher spatial resolution compared with their predecessors, enabling assessments of intra-urban NO_2 variation and identification of small NOx emissions sources.[39,40]

Here we investigate long-term trends of annual average NO_2 concentrations and associated pediatric asthma burdens in urban areas over the past two decades (2000-2019) globally. We first generate a new gridded global surface annual average NO_2 concentration dataset from 1990 to 2019 using satellite data from the Ozone Monitoring Instrument (OMI) to scale NO_2 concentrations estimated from a previously published land use regression (LUR) model[41] to different years. We then use epidemiological concentration-response relationships to estimate the temporal trend in urban NO_2-attributable pediatric asthma cases globally over the last two decades (2000-2019). Finally, we deconstruct the drivers of these trends to explore the influence of NO_2 versus demographic changes.

Methods

We integrated global environmental and demographic datasets available from different sources to generate new estimates of surface NO_2 concentrations and NO_2-attributable pediatric asthma incidence in cities globally. The analysis was done in Python (version 3.6.7).

NO_2 *concentrations*

We estimated surface annual average NO_2 concentrations at 0.0083 degree resolution (~1 km^2) in five-year increments from 1990-2010 and annually from 2010-2019. To begin, we used a previously published NO_2 concentration dataset for the average of 2010-2012, which used land use regression modeling with inputs from road networks and other land use variables, as well as satellite NO_2 column observations from SCIAMACHY and GOME-2.[4,41] We aggregated NO_2 concentrations from this dataset from its native 100m x 100m resolution globally to 0.0083 degree resolution, which is still a high enough resolution to avoid substantially underestimating NO_2-attributable asthma impacts.[19]

Due to the lack of ground measurements in rural areas, the Larkin et al.[41] NO_2 dataset is fine-tuned towards the urban areas and overestimates NO_2 concentrations in rural areas. We therefore applied the Larkin et al.[41] NO_2 concentrations in all 1km x 1km grid cells globally that are categorized as “urban” according to the Global Human Settlement Model grid,[42] as well as those grid cells that include major roadways[41]. For grid cells >5km away from roadways and in rural areas, we developed new NO_2 concentration estimates using NO_2 column observations from the OMI satellite instrument with some adjustments to fill spatial and temporal gaps in the OMI satellite record, and to estimate 24 hour averages from the early afternoon OMI overpass time. The datasets, correction factors, and evaluation against ground monitor observations are described in the Supplemental Material and in Table S1 and Figures S1 through S5.

While the global NO_2 concentration dataset is available for 1990-2019, the estimates for 1990 and 1995 have more uncertainty. Here, we use the results for 2000 to 2019 to explore trends and NO_2-attributable pediatric asthma incidence, as the long-term satellite observational record enhances confidence in results for this period.

NO_2-*attributable pediatric asthma incidence*

We estimated NO_2-attributable cases of pediatric asthma incidence for 2000-2019 using an epidemiologically-derived concentration response function, following the method used by Achakulwisut et al.[18] and Mohegh et al.[19], as shown in Equation 1:

Equation 1: $$Burden_{C,\ AG} = \sum_{Grid\ cells\ in\ C} Inc_{C,\ AG} \times Pop_{Grid\ cell\ (i,j),\ AG} \times (1 - e^{-\beta_{AG} X_{Grid\ cell\ (i,j)}})$$

where C is the country, AG is the age group, Inc is the baseline asthma incidence rate for the age group and country, Pop is the grid-cell population, β is the concentration response factor relating the NO_2 concentration with increased risk of asthma incidence, and X is the grid-cell annual average NO_2 concentration. We perform the health impact calculations at a spatial resolution close to the resolution of the population dataset (1km), since previous work indicates that 1km resolution achieves computational efficiency while still capturing co-location of concentrations and population at the city-scale. Therefore, all other datasets have been re-gridded to match it, including the concentration dataset at ~100m resolution and asthma baseline rates at the country/territory level). We assumed a theoretical minimum risk exposure level (TMREL) of 2 ppb annual average NO_2 concentration, and only estimated NO_2-attributable asthma incidence above that level. We applied a relative risk (RR) of 1.26 per 10ppb increase in annual average NO_2 concentration from Khreis et al.[16]

We use population estimates from Worldpop (Tatem 2017) in four different age groups (1-4, 5-9, 10-14, and 15-18 years old) from 2000-2019 at ~1km resolution. National baseline asthma incidence rates are from the Institute for Health Metrics and Evaluation's Global Burden of Disease (GBD) 2019 Study for the same age groups. Boundaries of urban areas are from the GHS-SMOD Urban Centre dataset which provides shapefiles of boundaries of over 13,000 urban clusters globally for the year 2015 (latest year).[42] We use the 2015 urban boundaries for all years of our analysis. Here, we consider grid-cells to be part of an "urban cluster" if they are included in "urban" and "sub-urban" areas in the GHS-SMOD dataset, which narrows the selection to areas with more than 300 people per km^2 that are part of clusters with more than 5000 population. We consider all other gridcells to be "rural". Regional definitions are consistent with the Global Burden of Disease 2019 Study.[1]

Drivers of change

To disentangle the contribution of exposure, population, and disease rates to NO_2-attributable pediatric asthma cases, we performed four sets of simulations: a control scenario, where we calculate the estimated asthma cases for each year, and three sets of scenarios in which we revert one contributing parameter back to the base year of 2000. Using a combination of these simulations, we estimate the contribution of each parameter in the overall changes in estimated asthma cases between 2000 and each year of analysis through 2019. The contribution of each parameter to that change in NO_2-attributable asthma cases between years is calculated using the formulas presented in the supplemental document. This method allows for calculating ratios for each parameter that add up to the scaling factor between the year 2019 and 2000, and due to its logarithmic nature, it is consistent with the original health impact function, which is a multiplication of three parameters. This approach is described in more detail in the Supplemental Material.

Role of the funding source

The funders of the study had no role in study design, data collection, data analysis, data interpretation, or writing of the report. SA and AM had full access to all the data in the study and had final responsibility for the decision to submit for publication.

Results

When averaged globally, urban annual average NO_2 concentrations decreased by 13% between 2000 and 2019 (Figure 1). We estimate that in 2000, the global urban population weighted average concentration was 12.2 ppb, it increased between 2006 and 2011, and then slowly declined from 2012 to a level of 10.6 ppb in 2019. However, these global trends mask steeper, and contrasting trends in different world regions. NO_2 concentrations in high-income cities were the highest among all regions in 2000, and remained above the global average throughout the time period, even after the steady, nearly monotonic decline of 35% in these cities from 2000 to 2019. In contrast, concentrations have risen in South Asia by 16% and in Sub-Saharan Africa by 11% over this period, though concentrations in these regions remain the lowest of cities in all other world regions in 2019. Cities in other world regions experienced only modest changes in NO_2 concentrations from 2000 to 2019. Even these large regional groupings of cities obscure contrasting temporal trends between sub-regions. For example, within the high-income region, concentrations dropped by nearly 53% in North America, but only by 35% and 39% in Western Europe and Australasia, respectively. In high-income Asia Pacific cities, concentrations rose dramatically in the 2000s and then declined steadily from 2005 to 2019, and are now at approximately the same level as in 2000. Another region with contrasting sub-regional trends is Central and Eastern Europe and Central Asia, where concentrations have dropped by a large amount in Central and Eastern Europe but have risen steadily in Central Asia. Similar trends can be seen when including all urban and rural areas together (Figure S7).

We estimate that 1.85 million new pediatric asthma cases were attributed to NO_2 pollution globally in 2019 (in both urban and rural areas, Figure S8), approximately 65% of which occurred in urban areas (Figure S9). Similar to concentrations, estimated NO_2-attributable pediatric asthma cases changed very little from 2000 to 2019 (Figure 2). Regional trends in estimated NO_2-attributable asthma incidence largely follow the NO_2 concentration trends, though with less cross-over in rankings between the world regions over time. For example, the high-income region had the most NO_2-attributable asthma incidence in 2000, and it still had the most in 2019, despite declining trends. Similarly, Central and Eastern Europe and Central Asia, South Asia, and Sub-Saharan Africa had the least NO_2-attributable asthma cases throughout 2000-2019, despite increasing trends over time. Sub-regional trends in NO_2-attributable asthma incidence show a similar pattern as sub-regional trends in NO_2 concentrations. Considering individual countries, the 2019 to 2000 ratio of urban NO_2-attributable asthma cases is relatively consistently positive throughout India, generally negative with increases in some areas within the United States and Western European countries, and very mixed within China, South American countries, and South Africa (Figure 3). While approximately two-thirds of NO_2-attributable asthma cases occurred in urban areas, there is wide variation across regions driven largely by differences in urban vs rural population in these regions (Figure S4).

The estimated trends in urban NO_2-attributable pediatric asthma incidence are driven by simultaneous and often competing changes in NO_2 concentrations, pediatric population size, and asthma incidence rates over time (Figure 4). We find that these drivers of the NO_2-attributable asthma trends are inconsistent globally, though some world regions show similar influences. No region that has experienced a decline in estimated NO_2-attributable asthma cases has done so without a drop in NO_2 concentrations. Similarly, all regions that experienced an increase in NO_2 concentrations saw an increase in estimated NO_2-attributable asthma cases. Australasia and high-income Asia Pacific are the only regions where concentrations, population, and disease rates all contribute to the overall decline in NO_2-attributable asthma cases. The opposite occurred In Central, South, and Southeast Asia, as well as in North Africa and the Middle East, where concentrations, population, and disease rates all contributed to an increasing trend in NO_2-attributable asthma cases. High-income North America, Western Europe, and several other regions experienced competing effects of reduced NO_2 concentrations but increases in asthma incidence rates and/or pediatric population size. These competing influences changed over time, such that declining concentrations have a larger influence over time in North America and Southern Latin America, while population growth becomes more of a factor in North Africa and Middle East and Southern Sub-Saharan Africa (Figure S10). Changing baseline pediatric asthma rates also influence the trends in some regions, in particular East Asia and Southern Sub-Saharan Africa.

Discussion

We found an emerging convergence in NO_2 concentrations globally, with high but declining concentrations in high-income countries that have regulated NO_2 and low but rising concentrations in other parts of the world where population is expanding. Estimated urban NO_2-attributable pediatric asthma incidence also appears to be beginning to converge globally, though with wider separation between world regions compared with regional average concentrations, driven by differences in population and asthma rates between countries. In no region did NO_2-attributable asthma cases decline without declining NO_2 concentrations, while population growth almost always contributed to rising trends in NO_2 asthma impacts. The influence of baseline pediatric asthma incidence rates was inconsistent between regions.

Our estimated NO_2 concentration trends are consistent with recent studies that used satellite data to investigate global NO_2 concentration trends during 2004-2018 for the U.S., Europe, China, India, and Japan[21,22,43]. Qu et al.[44] also showed a similar decrease in U.S. NO_2 concentrations based on ground observations, satellite data, and modeling outputs from 2006-2016, and Henneman et al.[25] showed a similar decrease using ground observations from 1980-2020.

Our estimate of 1.84 million NO_2-attributable new pediatric asthma cases globally (in both urban and rural areas) in 2019 is less than half of the 4.2 million found by Achakulwisut et al.[18] for 2015. Our estimates for India and the U.S. are 35% lower and 53% higher than our previous estimates, respectively[19]. Several factors explain this discrepancy. First, our new NO_2 concentration dataset corrects for a high NO_2 concentration bias in rural areas. This change results in lower contributions of NO_2 to asthma incidence in rural areas, particularly in countries with larger rural populations like India. Second, compared with previous GBD versions, GBD 2019 baseline asthma rates are much lower, except for high income areas such as the U.S. For example, the global baseline asthma incidence rate for people <20 years old in 2015 (the year analyzed by Mohegh et al.[19]) decreased from 1055 to 828 cases per 100,000 in the GBD 2017 (GBD 2017) vs. GBD 2019 Study (GBD 2019). This difference is even larger in China and India, where pediatric asthma incidence rates in the GBD 2019 Study were ~72% of their value in the GBD 2017 Study. U.S. baseline pediatric asthma incidence rates increased from 1257 to 2750 cases per 100,000 in the GBD 2017 vs. GBD 2019 Study. Changes in baseline asthma rates have approximately proportional effects on estimated NO_2-attributable pediatric asthma cases. Finally, as we have shown, NO_2 concentrations are changing rapidly in different directions depending on the region and city, with the same directional effect on estimated NO_2-attributable pediatric asthma cases.

While we sought to create a new NO_2 dataset that leverages the advantages of different data sources, our new NO_2 concentrations are still uncertain. First, many cities are still lacking ground NO_2 monitors, limiting our ability to calibrate and evaluate concentrations in these regions.[41] Urban NO_2 concentrations therefore have more certainty in North America, Europe, and Asia, compared with Africa and South America. Second, rural NO_2 concentrations are uncertain in all regions globally due to the disproportionate location of ground monitors in urban areas. Third, our approach for scaling NO_2 concentrations from the 2010-2012 average LUR model to other years assumes that the land use predictors of that regression model are unchanged over time. This assumption is likely supported by slow changes in road density and volume and urban form from one year to the next, but over the two decades time frame explored here, some land use evolution is likely. The directional impact of these uncertainties and limitations on results is currently unknown.

Estimated NO_2-attributable asthma incidence is heavily influenced by baseline disease rates, which vary considerably within individual countries.[45] While we used national pediatric asthma rates, asthma prevalence differs between urban and rural areas. Living in urban areas has been associated with increased risk of asthma prevalence in low- and middle-income countries[46] and asthma-related emergency department visits and hospitalizations in the U.S.[47] Our method also does not capture temporal trends in asthma rates in cities specifically, which may differ from the broader national rate changes. If asthma prevalence tends to be higher in urban areas compared with national averages, we may have underestimated NO_2-attributable asthma cases.

Despite these uncertainties and limitations, our results demonstrate the important influence of combustion-related air pollution on children's health in cities globally. In places that have effective air quality management programs, NO_2 concentrations have been trending downward for decades, with benefits for improved children's respiratory health. Even with these improvements, the current levels of NO_2 contribute substantially to pediatric asthma incidence, highlighting that mitigating air pollution should be a critical element of children's public health strategies. For cities that have not benefited from strong local or national-scale air quality management programs, the experience of cities that have such programs demonstrates that addressing combustion-related air pollution can lead to dramatic improvements in air quality and public health over short time frames. These air quality improvements can be achieved through either end-of-pipe emission control technologies or avoiding the combustion in the first place, which would have additional benefits from reduced greenhouse gas emissions.

Our study also highlights the value of satellite remote sensing and statistical models for tracking NO_2 pollution and for environmental health surveillance at local, national, and global scales. The combination of methods offers strengths beyond what is possible from each technique alone: a long and consistent observational record of NO_2 column densities from satellite remote sensing with the high spatial resolution of the surface concentration predictions from the LUR model. Future studies may seek to leverage these data sources and others, including mobile monitoring, distributed networks of ground sensors, and chemical transport models, to further improve upon the accuracy and spatiotemporal resolution of NO_2 concentration estimates. Further, our study shows the importance of considering not just concentrations, but how demographics change over time, for understanding air pollution health risks. Improved and more widely accessible information about disease rates, and capturing population distribution and movement, will enable more accurate and highly resolved air pollution health impact assessments.

References

1 GBD. Global Burden of Disease (GBD 2019) | Institute for Health Metrics and Evaluation. 2020. DOI:10.6069/P5WM-5A36.

2 Stavrakou T, Müller J-F, Boersma KF, De Smedt I, van der A RJ. Assessing the distribution and growth rates of NOx emission sources by inverting a 10-year record of NO_2 satellite columns. *Geophys Res Lett* 2008; **35**. DOI:10.1029/2008GL033521.

3 Bechle MJ, Millet DB, Marshall JD. Effects of Income and Urban Form on Urban NO_2 : Global Evidence from Satellites. *Environ Sci Technol* 2011; **45**: 4914–9.

4 Geddes JA, Martin R V., Boys BL, van Donkelaar A. Long-Term Trends Worldwide in Ambient NO 2 Concentrations Inferred from Satellite Observations. *Environ Health Perspect* 2016; **124**: 281–9.

5 Bechle MJ, Millet DB, Marshall JD. Does urban form affect urban NO_2 Satellite-based evidence for more than 1200 cities. *Environ Sci Technol* 2017; **51**: 12707–16.

6 McDuffie EE, Smith SJ, O'Rourke P, *et al.* A global anthropogenic emission inventory of atmospheric pollutants from sector- and fuel-specific sources (1970–2017): an application of the Community Emissions Data System (CEDS). *Earth Syst Sci Data* 2020; **12**: 3413–42.

7 Anenberg SC, Miller J, Minjares R, *et al.* Impacts and mitigation of excess diesel-related NOx emissions in 11 major vehicle markets. *Nature* 2017; **545**: 467–71.

8 Stohl A, Aamaas B, Amann M, *et al.* Evaluating the climate and air quality impacts of short-lived pollutants. *Atmos Chem Phys* 2015; **15**: 10529–66.

9 Crippa M, Guizzardi D, Muntean M, *et al.* Gridded emissions of air pollutants for the period 1970--2012 within EDGAR v4.3.2. *Earth Syst Sci Data* 2018; **10**: 1987–2013.

10 Duncan BN, Yoshida Y, De Foy B, *et al.* The observed response of Ozone Monitoring Instrument (OMI) NO_2 columns to NOx emission controls on power plants in the United States: 2005-2011. *Atmos Environ* 2013; **81**: 102–11.

11 Silvern RF, Jacob DJ, Mickley LJ, *et al.* Using satellite observations of tropospheric NO_2 columns to infer long-term trends in US NOx emissions: the importance of accounting for the free tropospheric NO_2 background. *Atmos Chem Phys* 2019; **19**: 8863–78.

12 Dix B, Bruin J, Roosenbrand E, *et al.* Nitrogen Oxide Emissions from U.S. Oil and Gas Production: Recent Trends and Source Attribution. *Geophys Res Lett* 2020; **47**: 2019GL085866.

13 Goldberg DL, Anenberg SC, Griffin D, McLinden CA, Lu Z, Streets DG. Disentangling the Impact of the COVID-19 Lockdowns on Urban NO_2 From Natural Variability. *Geophys Res Lett* 2020; **47**. DOI:10.1029/2020GL089269.

14 Perez L, Lurmann F, Wilson J, *et al.* Near-Roadway Pollution and Childhood Asthma: Implications for Developing "Win–Win" Compact Urban Development and Clean Vehicle Strategies. *Environ Health Perspect* 2012; **120**: 1619–26.

15 Gauderman WJ, Avol E, Lurmann F, *et al.* Childhood Asthma and Exposure to Traffic and Nitrogen Dioxide. *Epidemiology* 2005; **16**: 737–43.

16 Khreis H, Kelly C, Tate J, Parslow R, Lucas K, Nieuwenhuijsen M. Exposure to traffic-related air pollution and risk of development of childhood asthma: A systematic review and meta-analysis. *Environ Int* 2017; **100**: 1–31.

17 Anenberg SC, Henze DK, Tinney V, *et al.* Estimates of the Global Burden of Ambient PM2.5, Ozone, and NO_2 on Asthma Incidence and Emergency Room Visits. *Environ Health Perspect* 2018; **126**: 107004.

18 Achakulwisut P, Brauer M, Hystad P, Anenberg SC. Global, national, and urban burdens of paediatric asthma incidence attributable to ambient NO_2 pollution: estimates from global datasets. *Lancet Planet Heal* 2019. DOI:10.1016/S2542-5196(19)30046-4.

19 Mohegh A, Goldberg DL, Achakulwisut P, Anenberg SC. Sensitivity of estimated NO_2-attributable pediatric asthma incidence to grid resolution and urbanicity. *Environ Res Lett* 2020; published online Nov 26. DOI:10.1088/1748-9326/abce25.

20 Lamsal LN, Duncan BN, Yoshida Y, *et al.* U.S. NO_2 trends (2005-2013): EPA Air Quality System (AQS) data versus improved observations from the Ozone Monitoring Instrument (OMI). *Atmos Environ* 2015; **110**: 130–43.

21 Miyazaki K, Eskes H, Sudo K, Folkert Boersma K, Bowman KW, Kanaya Y. Decadal changes in global surface NOxemissions from multi-constituent satellite data assimilation. *Atmos Chem Phys* 2017; **17**: 807–37.

22 Georgoulias AK, van der A RJ, Stammes P, Boersma KF, Eskes HJ. Trends and trend reversal detection in 2 decades of tropospheric NO_2 satellite observations. *Atmos Chem Phys* 2019; **19**: 6269–94.

23 Tong DQ, Lamsal L, Pan L, *et al.* Long-term NOx trends over large cities in the United States during the great recession: Comparison of satellite retrievals, ground observations, and emission inventories. *Atmos Environ* 2015; **107**: 70–84.

24 Kharol SK, Martin R V., Philip S, *et al.* Assessment of the magnitude and recent trends in satellite-derived ground-level nitrogen dioxide over North America. *Atmos Environ* 2015; **118**: 236–45.

25 Henneman LRF, Shen H, Hogrefe C, Russell AG, Zigler CM. Four Decades of United States Mobile Source Pollutants: Spatial–Temporal Trends Assessed by Ground-Based Monitors, Air Quality Models, and Satellites. *Environ Sci Technol* 2021; : acs.est.0c07128.

26 Goldberg DL, Lu Z, Oda T, *et al.* Exploiting OMI NO<inf>2</inf> satellite observations to infer fossil-fuel CO<inf>2</inf> emissions from U.S. megacities. *Sci Total Environ* 2019; **695**. DOI:10.1016/j.scitotenv.2019.133805.

27 Zhang R, Wang Y, Smeltzer C, Qu H, Koshak W, Folkert Boersma K. Comparing OMI-based and EPA AQS in situ NO_2 trends: towards understanding surface NOx emission changes. *Atmos Meas Tech* 2018; **11**: 3955–67.

28 Curier RL, Kranenburg R, Segers AJS, Timmermans RMA, Schaap M. Synergistic use of OMI NO_2 tropospheric columns and LOTOS-EUROS to evaluate the NOx emission trends across Europe. *Remote Sens Environ* 2014; **149**: 58–69.

29 Zara M, Boersma KF, Eskes H, *et al.* Reductions in nitrogen oxides over the Netherlands between 2005 and 2018 observed from space and on the ground: decreasing emissions and increasing O3

indicate changing NOx chemistry. *Atmos Environ X* 2021; : 100104.

30 Itahashi S, Yumimoto K, Kurokawa J, *et al.* Inverse estimation of NOx emissions over China and India 2005–2016: contrasting recent trends and future perspectives. *Environ Res Lett* 2019; **14**: 124020.

31 Barkley PM, González Abad G, Kurosu PT, Spurr R, Torbatian S, Lerot C. OMI air-quality monitoring over the Middle East. *Atmos Chem Phys* 2017; **17**. DOI:10.5194/acp-17-4687-2017.

32 De Foy B, Lu Z, Streets DG. Satellite NO_2 retrievals suggest China has exceeded its NOx reduction goals from the twelfth Five-Year Plan. *Sci Rep* 2016; **6**: 1–9.

33 Liu F, Beirle S, Zhang Q, *et al.* NOx emission trends over Chinese cities estimated from OMI observations during 2005 to 2015. *Atmos Chem Phys* 2017; **17**: 9261–75.

34 Zheng B, Tong D, Li M, *et al.* Trends in China's anthropogenic emissions since 2010 as the consequence of clean air actions. *Atmos Chem Phys* 2018; **18**: 14095–111.

35 Leue C, Wenig M, Wagner T, Klimm O, Platt U, Jähne B. Quantitative analysis of NOx emissions from Global Ozone Monitoring Experiment satellite image sequences. *J Geophys Res Atmos* 2001; **106**: 5493–505.

36 VanDerA RJ, Eskes HJ, Boersma KF, *et al.* Trends, seasonal variability and dominant NOx source derived from a ten year record of NO_2 measured from space. *J Geophys Res Atmos* 2008; **113**: 1–12.

37 Duncan BN, Lamsal LN, Thompson AM, *et al.* A space-based, high-resolution view of notable changes in urban NOx pollution around the world (2005-2014). *J Geophys Res Atmos* 2016; **121**: 976–96.

38 Anenberg SC, Bindl M, Brauer M, *et al.* Using Satellites to Track Indicators of Global Air Pollution and Climate Change Impacts: Lessons Learned From a NASA-Supported Science-Stakeholder Collaborative. *GeoHealth* 2020; **4**. DOI:10.1029/2020GH000270.

39 Griffin D, Zhao X, McLinden CA, *et al.* High-Resolution Mapping of Nitrogen Dioxide With TROPOMI: First Results and Validation Over the Canadian Oil Sands. *Geophys Res Lett* 2019; **46**: 1049–60.

40 Goldberg DL, Anenberg SC, Kerr GH, Mohegh A, Lu Z, Streets DG. TROPOMI NO_2 in the United States: A detailed look at the annual averages, weekly cycles, effects of temperature, and correlation with surface NO_2 concentrations. *Earth's Futur* 2021; : e2020EF001665.

41 Larkin A, Geddes JA, Martin R V., *et al.* Global Land Use Regression Model for Nitrogen Dioxide Air Pollution. *Environ Sci Technol* 2017; **51**: 6957–64.

42 Pesaresi M, Florczyk A, Schiavina M, Melchiorri M, Maffeninni L. GHS-SMOD R2019A - GHS settlement layers, updated and refined REGIO model 2014 in application to GHS-BUILT R2018A and GHS-POP R2019A, multitemporal (1975-1990-2000-2015) - Datasets. 2019. DOI:10.2905/42E8BE89-54FF-464E-BE7B-BF9E64DA5218.

43 Jamali S, Klingmyr D, Tagesson T. Global-Scale Patterns and Trends in Tropospheric NO_2 Concentrations, 2005–2018. *Remote Sens* 2020; **12**: 3526.

44 Qu Z, Henze DK, Cooper OR, Neu JL. Impacts of global NOx inversions on NO_2 and ozone

simulations. *Atmos Chem Phys* 2020; **20**: 13109–30.

45 Khreis H, Alotaibi R, Horney J, McConnell R. The impact of baseline incidence rates on burden of disease assessment of air pollution and onset childhood asthma: analysis of data from the contiguous United States. *Ann Epidemiol* 2021; **53**: 76--88.e10.

46 Rodriguez A, Brickley E, Rodrigues L, Normansell RA, Barreto M, Cooper PJ. Urbanisation and asthma in low-income and middle-income countries: a systematic review of the urban–rural differences in asthma prevalence. *Thorax* 2019; **74**: 1020 LP-- 1030.

47 Keet CA, Matsui EC, McCormack MC, Peng RD. Urban residence, neighborhood poverty, race/ethnicity, and asthma morbidity among children on Medicaid. *J Allergy Clin Immunol* 2017; **140**: 822–7.

Figure captions

Figure 1. Trends in annual average NO_2 surface concentrations in urban areas in various world regions. The figure presents regional average concentrations aggregated for GBD super regions in form of NO_2 concentrations (main panel) and aggregated results for GBD regions in each super region in form of relative changes from the year 2000 (side panels). Regional definitions are shown in Figure S5. China is included in East Asia and India is included in South Asia. H.I. = High Income; L.A.C. = Latin America & Caribbean; S.S.A. = Sub-Saharan Africa; N.A.,M.E. = North Africa and Middle East; S.A. = South Asia; SE.A., E.A., O. = Southeast Asia, East Asia, and Oceania; C.E., E.E., C.A. = Central Europe, Eastern Europe, and Central Asia.

Figure 2. Trends in estimated urban NO_2-attributable pediatric asthma incidence in each super-region (absolute magnitude, main panel) and sub-region (relative changes from 2000, side panels). The legends are the same as Figure 1.

Figure 3. Relative changes in estimated NO_2-attributable pediatric asthma incidence between 2000 and 2019 globally (including both urban and rural areas). Lack of color indicates no NO_2-attributable pediatric asthma incidence as NO_2 concentrations were <2 ppb, the low concentration threshold for estimating attributable asthma incidence.

Figure 4. Contribution of population, baseline asthma rates, and NO_2 concentrations to changes in estimated NO_2-attributable pediatric asthma incidence between the year 2000 and 2019 for each sub-region. Since meteorological factors can influence comparisons of concentration contributions when comparing two years, we show contributions by year for several regions in Figure S3. Percentage labels indicate the net change.


Super regions
High Income
Latin America & Caribbean
Sub-Saharan Africa
North Africa and Middle East
South Asia
S.E./E. Asia and Oceania
C./E. Europe, and C. Asia
NO_2 (ppb)
2000
2005
2010
2015
2019
Global
H.I., Southern Latin America
H.I., Western Europe
H.I., High-income North America
H.I., Australasia
H.I., High-income Asia Pacific
L.A.C, Central Latin America
L.A.C, Tropical Latin America
L.A.C, Andean Latin America
L.A.C, Caribbean
S.S.A, Southern Sub-Saharan Africa
S.S.A, Western Sub-Saharan Africa
S.S.A, Central Sub-Saharan Africa
S.S.A, Eastern Sub-Saharan Africa
N.A., M.E., North Africa and Middle East
S.A., South Asia
SE.A., E.A., O., East Asia
SE.A., E.A., O., Southeast Asia
SE.A., E.A., O., Oceania
C.E., E.E., C.A., Central Asia
C.E., E.E., C.A., Eastern Europe
C.E., E.E., C.A., Central Europe

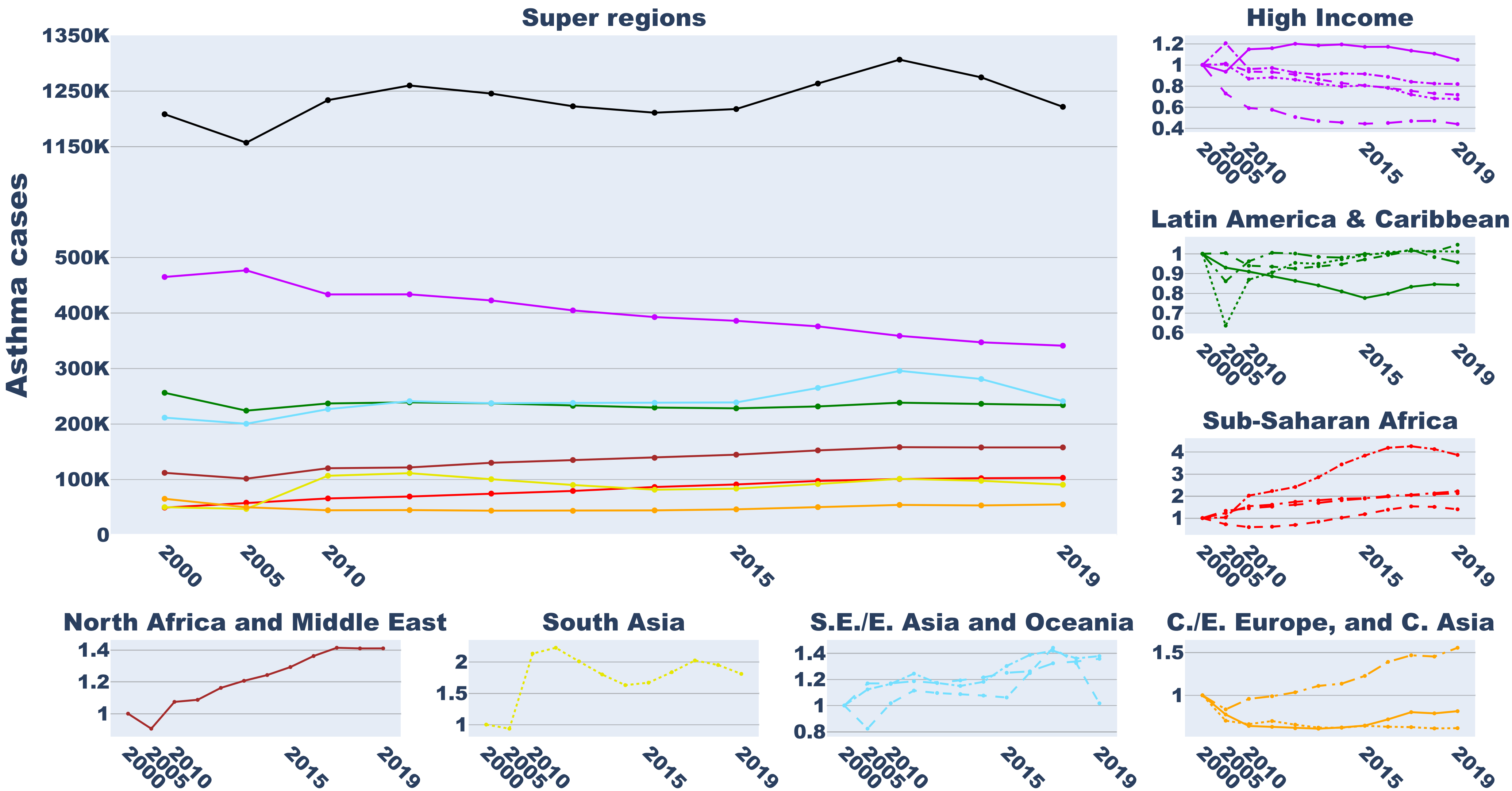

Super regions
Asthma cases
1350K
1250K
1150K
500K
400K
300K
200K
100K
0
2000
2005
2010
2015
2019
High Income
Latin America & Caribbean
Sub-Saharan Africa
North Africa and Middle East
South Asia
S.E./E. Asia and Oceania
C./E. Europe, and C. Asia

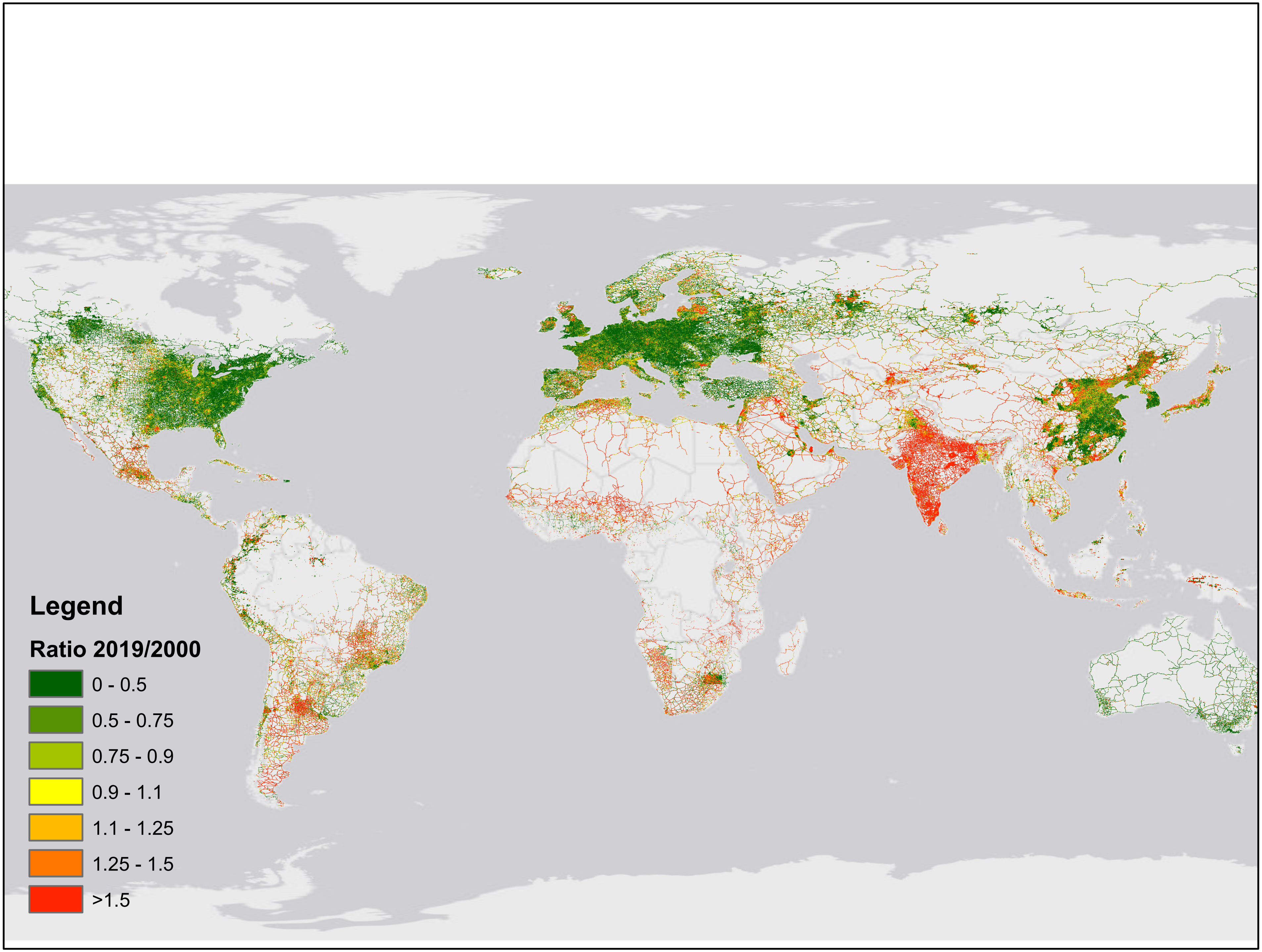
Legend
Ratio 2019/2000
0 - 0.5
0.5 - 0.75
0.75 - 0.9
0.9 - 1.1
1.1 - 1.25
1.25 - 1.5
>1.5

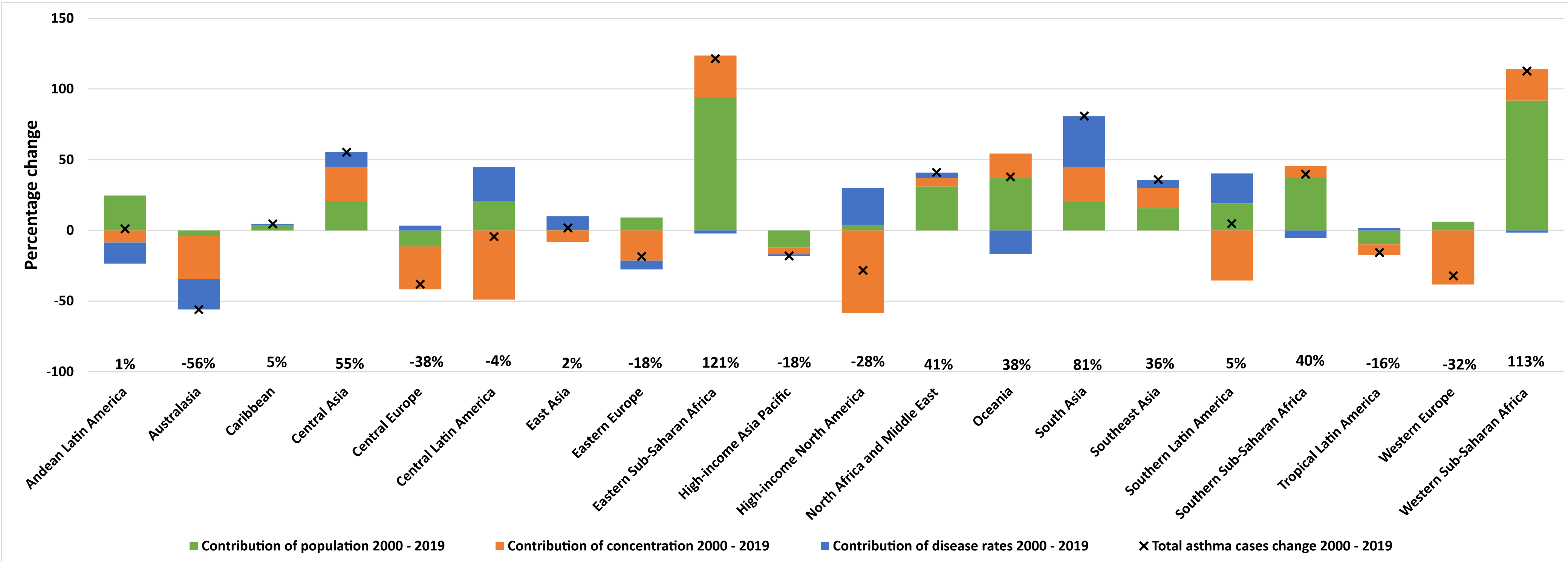

Percentage change
150
100
50
0
-50
-100
1%
-56%
5%
55%
-38%
-4%
2%
-18%
121%
-18%
-28%
41%
38%
81%
36%
5%
40%
-16%
-32%
113%
Andean Latin America
Australasia
Caribbean
Central Asia
Central Europe
Central Latin America
East Asia
Eastern Europe
Eastern Sub-Saharan Africa
High-income Asia Pacific
High-income North America
North Africa and Middle East
Oceania
South Asia
Southeast Asia
Southern Latin America
Southern Sub-Saharan Africa
Tropical Latin America
Western Europe
Western Sub-Saharan Africa
Contribution of population 2000 - 2019
Contribution of concentration 2000 - 2019
Contribution of disease rates 2000 - 2019
Total asthma cases change 2000 - 2019